ALT 12
Advanced Laser Technologies
2 – 6 September 2012, Thun, Switzerland

ALT 12
c/o Bern University of Applied Sciences
Engineering and Information Technology
Pestalozzistrasse 20, CH-3400 Burgdorf
info@alt12.org, www.alt12.org
0041 (0) 34 426 42 06

UV PICOSECOND-LASER INDUCED BULK MODIFICATIONS AND LUMINESCENCE IN SINGLE-CRYSTAL DIAMOND

Authors:

S.M. Pimenov, A.A. Khomich, I.I. Vlasov, E.V. Zavedeev, B. Neuenschwander, B. Jäggi, V. Romano

DOI: 10.12684/alt.1.50

Corresponding author: S.M. Pimenov

e-mail: pimenov@nsc.gpi.ru

UV Picosecond-Laser Induced Bulk Modifications and Luminescence in Single-Crystal Diamond

S.M. Pimenov[1], A.A. Khomich[1], I.I. Vlasov[1], E.V. Zavedeev[1],
B. Neuenschwander[2], B. Jäggi[2], V. Romano[2]

[1]Natural Sciences Center, Prokhorov General Physics Institute, Moscow 119991, Russia
[2]Bern University of Applied Sciences, Engineering & Information Technology, Burgdorf CH-3400, Switzerland

Abstract

Bulk laser-graphitized microstructures have been fabricated in type IIa single-crystal 1.2-mm-thick diamond plates by UV laser irradiation with 10-ps pulses at λ=355 nm wavelength. It is found that the crystallographic-plane-dependent character of structural modifications in the bulk is influenced by the laser wavelength and the direction of the laser beam incidence relative to a given crystallographic direction (<100> or <110>) in the diamond plates. High-order Stokes Raman lasing is observed during UV laser irradiation and bulk modifications of single-crystal diamond. It is shown that the formation of bulk microstructures results in dramatic changes in the behavior of the stimulated Raman scattering in diamond. The formation and migration of the 3H defects (self-interstitial related centers) is also found to take place in the course of bulk microstructuring with UV ps-pulses. Important limitations of the bulk microstructuring caused by high internal stresses in laser-modified regions resulting in 'uncontrollable' damage of the diamond single crystals are discussed.

Introduction

Recently we have demonstrated high-rate bulk modification and microstructuring of type IIa single-crystal mm-thick diamond plates using a picosecond MOPA (master-oscillator power-amplifier) laser system with 10-ps pulses at λ=532 nm wavelength [1]. The fundamental result of the studies of ref. [1] is related to the findings of (i) the crystallographic-plane-dependent character of bulk modifications and (ii) appearance of 3H luminescence in ps-laser-irradiated diamond, which are of great interest for understanding the mechanisms of ultrafast phase transitions and the 3H center formation during ps-laser irradiation. The findings are also of importance for applications dealing with laser microstructuring in the bulk of single crystals to be controlled by the strength anisotropy of diamond.

In this paper, we report on the bulk modifications and luminescence induced in single-crystal diamond by UV ps-laser irradiation using the 3rd laser harmonic (λ=355 nm) of a picosecond MOPA system – the DUETTO™ laser system (which generates pulses of 10-ps duration) [2,3]. From the experimental data obtained, emphasis is placed on (i) effects of the laser wavelength and direction of the laser beam incidence on the crystallographic-plane-dependent bulk modifications, (ii) generation of stimulated Raman scattering (SRS) in diamond under UV ps-laser irradiation and the SRS behavior after formation of bulk microstructures, and (iii) structure transformation of diamond and formation of the 3H defect centers as a result of the bulk microstructuring with UV ps-pulses. In addition, experimental data of laser damage in the bulk of diamond, and results of modeling and estimation of internal stresses in the system 'graphitized cylinder-in-diamond' are presented and discussed.

Experimental

The type IIa CVD single crystal (SC) diamond plates of 6.0x1.7x1.2 mm size, with mechanically polished {100} growth faces and {110} side faces, nitrogen content [N] < 1 ppm (from Element Six Ltd [4]), were used as the samples for UV ps-laser microstructuring. The optical transmission spectrum of a CVD single crystal diamond sample is shown in Figure 1, demonstrating high optical quality of diamond and high transmission values at two laser wavelengths (λ=355 nm and λ=532 nm) used in ps-laser microstructuring experiments.

The UV laser beam was focused onto the rear side of the diamond plates; the pulse energy was varied from 0.1 μJ to 6 μJ, and the pulse repetition rate – from 10 to 50 kHz. A video imaging system was applied for real-time observation of the growth of a laser-modified region in the bulk of diamond in the course of multipulse laser irradiation as described and demonstrated in ref. [1]. In addition, UV ps-laser induced photoluminescence (PL) spectra over the range of 350-1000 nm were recorded during laser irradiation; the PL setup provided measurements perpendicularly to the laser beam through a polished side face of the diamond plate. The UV laser-induced PL due to the nitrogen-vacancy (NV) defects [5] (the NV luminescence) is

observed at wavelengths of 575-750 nm, which makes the UV laser beam 'visible' during irradiation of the diamond crystals. Figure 2 shows the laser beam path visible as a 'red line' across the diamond plate and the NV luminescence spectrum measured in the course of ps-laser multipulse irradiation.

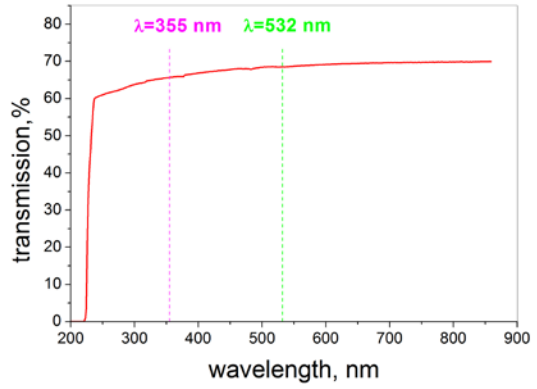

Figure 1
Optical transmission spectrum of a CVD single-crystal diamond plate used in the ps-laser microstructuring experiments. Dashed lines show the transmission values at the 3rd (λ=355 nm) and 2nd (λ=532 nm) laser harmonics of the ps-laser system.

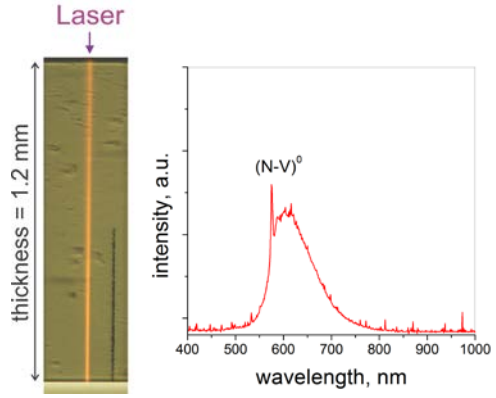

Figure 2
Optical image (left) of the UV laser beam passing through a 1.2-mm-thick diamond plate, and PL spectrum (right) recorded during irradiation with UV ps-laser pulses (λ=355 nm).

The microstructural properties of the UV laser-modified regions were examined using micro-Raman and PL spectroscopy at the 488 nm excitation wavelength. The Raman and PL spectra were measured on the rear side of the diamond plates as described elsewhere [1]; the spectra were recorded at room temperature.

Results

Crystallographic-Plane-Dependent Bulk Modifications in Single-Crystal Diamond

Using the techniques described above, bulk microstructures have been fabricated in 1.2-mm-thick single-crystal diamond plates at different pulse energies (E) and pulse repetition rates (f) of the UV ps-laser. Figure 3 displays an optical image of bulk microstructures fabricated at the pulse energies varied from E=0.2 to 1.8 μJ (from left to right in Figure 3), pulse repetition rate f=10 kHz, and translation speed V_z=0. The microstructures were fabricated at 50 μm spacing. The focal plane of a laser beam was located at the back side (BS) of the diamond plate and the laser beam radius was r=5 μm. The threshold of the structure formation at the BS was E=0.2 μJ; the length of a bulk structure formed was found to increase with the pulse energy similar to the data on fs-laser microstructuring in the bulk of diamond [6,7]. In addition, features of a bulk microstructure formation are shown with a higher resolution in Figure 4, which are characteristic of UV ps-laser irradiation at the beam incidence along the [100] direction in the crystal.

Figures 3 and 4 evidence that the crystallographic-plane-dependent structural modifications in the bulk are initiated along {111} planes during irradiation with UV laser pulses. These bulk modifications seem to be more distinctly pronounced in laser microstructuring of diamond with UV ps pulses than with the ps pulses at λ=532 nm (reported previously in ref. [1]).

To give an example, the structure formed at the pulse energy of E=1.8 μJ (first on the right in Figure 3) clearly shows that the structure transformation starts at the BS and propagates along {111} planes (i.e. at a fixed angle of 54.5° to the {100}-aligned diamond surface [1]). Also, 'zig-zag'-like structures in Figure 4 suggest that the UV ps-laser-induced phase transformation starts along the {111} planes (known as the planes of the lowest strength in diamond crystals [8]) and propagates normally to these planes. Different character of the onset of structure transformation on the BS might be caused by local surface properties of the polished diamond which undergoes (during polishing) an sp^3–sp^2 order–disorder transition resulting in an amorphous adlayer at the surface [9].

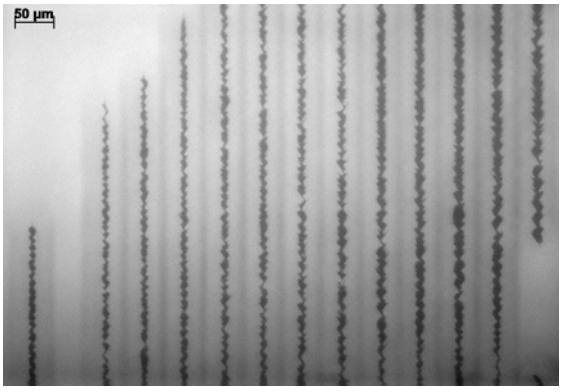

Figure 3
Optical image of UV ps-laser-induced microstructures fabricated at pulse energies varied from E=0.2 to 1.8 μJ (from left to right), the pulse repetition rate f=10 kHz, and translation speed V_z=0. Bottom boundary of the image corresponds to the back side of the diamond plate.

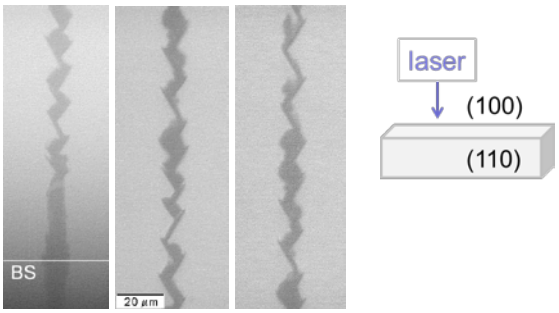

Figure 4
Optical images of three different parts of a microstructure grown from the back side into the bulk (to ~ 0.5 mm depth from the BS) during UV ps-laser irradiation at E=2 μJ, f=50 kHz, V_z=0. The laser beam was incident along [100] direction.

In all previous experiments on the bulk microstructuring of diamond crystals with ultra-short laser pulses [1,7] a laser beam was incident normally to the polished {100} top faces. So, the question emerged whether it would be possible to control microstructuring along the {111} planes by changing the angle of incidence of the laser beam?

Figure 5 shows the results of microstructuring with the UV laser beam incident normally to the side face of the diamond plate in the [110] direction.

Figure 5
Optical image of three bulk microstructures fabricated by UV ps-laser irradiation at E=1.4, 1.8 and 2.0 μJ (from left to right), f=50 kHz, V_z=0. The laser beam was incident along [110] direction.

Comparing images in Figure 5 and Figure 4, one can see that changing the direction of incidence of the laser beam (from the [100] to the [110] direction) strongly influences the microstructure formation in the bulk of diamond. The bulk microstructures shown in Figure 5 are viewed from the [100] direction, so the data of viewing from other directions is needed to get a real '3D' image of the produced microstructures and to clarify the effect of laser beam incidence on crystallographic-plane-dependent bulk modifications in single-crystal diamond.

Structure Transformation and 3H Luminescence

Results of microstructural studies of the UV ps-laser-modified diamond and 3H luminescence are presented in Figures 6 and 7. Figure 6 displays Raman spectra of three microstructures produced at different pulse energies E=0.5, 0.9 and 1.4 μJ, and pulse repetition rate f=10 kHz; the spectra were measured at the back side of the sample shown in Figure 3. The Raman spectra are characterized by two broad bands at 1350 cm^{-1} (D band) and 1580 cm^{-1} (G band) which are typical of amorphous carbon structures; the spectra resemble those of tetrahedral amorphous carbon (ta-C) films with high sp^3 content after annealing at 1000-1100°C [10]. A weak diamond peak at 1332 cm^{-1} is also observed in the spectra, which indicates either a presence of a thin 'diamond cap' at the BS surface of laser spots or a composite 'diamond-amorphous cabon' structure of the laser-modified diamond.

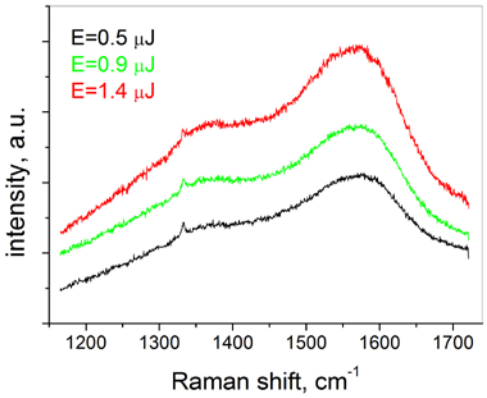

Figure 6
Raman spectra of the microstructures produced at different pulse energies E=0.5, 0.9 and 1.4 μJ, and f=10 kHz; the spectra were measured at the BS of the sample shown in Figure 3.

PL spectra measured between different spots (at a half the distance between two adjacent microstructures) on the BS of the diamond plate are shown in Figure 7. The presence of a PL line at 504 nm, attributed to PL from the 3H center [5,11], confirms that the formation and migration of the 3H defects (self-interstitial related centers) take place in the course of bulk microstructuring with UV ps-pulses. It should be emphasized that the 3H luminescence was not detected during UV ps-laser irradiation of the diamond crystals, see Figure 2 and Figures 8 and 9 below. This fact agrees with the previous results and suggestion of a charged state of the 3H center [5].

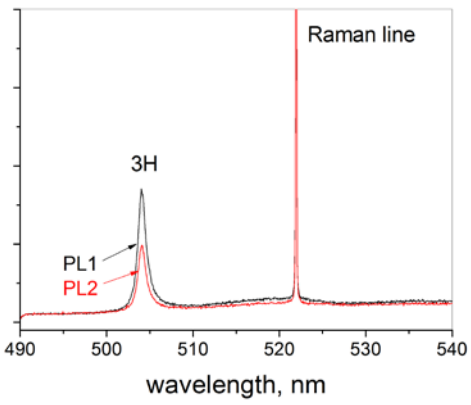

Figure 7
PL spectra measured between different spots on the BS of the sample shown in Figure 3: PL1 – between spots 4 and 5; PL2 – between spots 11 and 12. Excitation wavelength 488 nm.

Stimulated Raman Scattering in Single-Crystal Diamond under UV ps-laser irradiation

Photoluminescence spectra recorded in the course of UV laser irradiation have enabled important data on the ps-laser induced processes in the bulk of diamond to be obtained. In addition to the NV luminescence discussed above, stimulated Raman scattering (SRS) is generated in the diamond crystals under UV ps-laser irradiation. With increasing pulse energy the SRS lasing has been observed at the 1st Stokes, 2nd Stokes, and 3rd Stokes wavelengths – λ_{1S}=372.6 nm, λ_{2S}=392 nm, λ_{3S}=413.7 nm, respectively, as shown in Figure 8. The irradiation conditions for the SRS generation were similar to those in Figure 5 except for the higher pulse energies used (up to 5 μJ) which did not result yet in a structure formation at the rear side of the crystal. This was due to focusing a laser beam 0.5 mm beyond the crystal, so that the beam radius was increased from 5 μm to ~15 μm and the incident fluence was lowered. The PL setup provided spectra measurements perpendicularly to the laser beam, different from standard schemes using forward scattering geometry [12,13]; a local volume in the bulk at ~500 μm from the back side was probed to get the resulting spectra.

The formation of a bulk microstructure in diamond was found to result in dramatic changes in the PL spectra and SRS lasing. Figure 9 shows that the intensities of the scattered laser light and all Stokes components (especially, the 1st Stokes) are strongly increased after a short-length microstructure is formed at the back side of the crystal. During repeated tests at average powers up to 300 mW (E=6 μJ, f=50 kHz) the SRS behavior was quite stable and the length of the bulk microstructure only slightly increased.

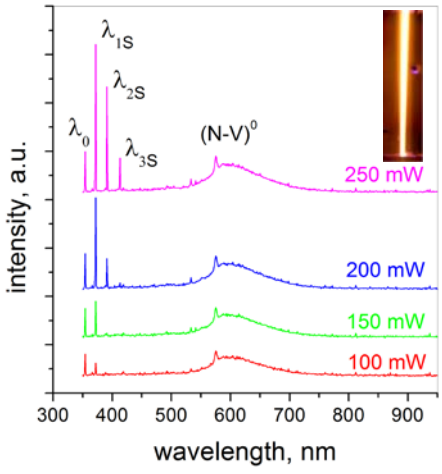

Figure 8
PL spectra measured during UV ps-laser irradiation of the crystal at different pulse energies (from 0.5 to 5 μJ) and f=50 kHz, V_z=0. λ_0=355 nm is the laser wavelength. The generated 1st Stokes, 2nd Stokes, and 3rd Stokes wavelengths are λ_{1S}=372.6 nm, λ_{2S}=392 nm, λ_{3S}=413.7 nm. An inset shows an optical image of the UV laser beam of 250 mW passing through the diamond plate.

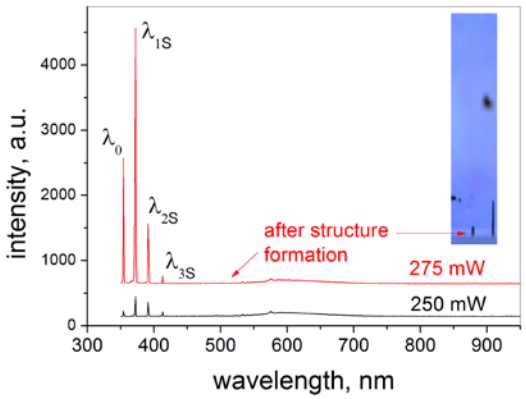

Figure 9
PL spectra measured during UV ps-laser irradiation before and after a microstructure formation at the BS of the diamond plate. The pulse energy/average power are 5 μJ/250 mW and 5.5 μJ/ 275 mW, respectively; f=50 kHz, V_z=0. The 'red' spectrum is shifted upwards for clarity. An inset shows an optical image of a short-length microstructure formed at the BS.

Recent studies of the SRS in diamond [13-17] showed high potential of CVD diamond single-crystals for the development of efficient diamond Raman lasers. The results of this paper give new information on the SRS in diamond under UV ps-laser pumping and SRS behavior after formation of bulk microstructures and are important for novel Raman laser applications of CVD SC diamond.

Laser Damage in the Bulk of Diamond

Laser microstructuring in the bulk of diamond is of interest only if the internal stresses, generated as a result of the bulk modification (graphitization), do not cause local mechanical damage in the crystals. It is well known that when the fracture strength is exceeded, microcracks of certain lengths grow catastrophically [18]. Indeed, in the experiments we observed such a catastrophic crack growth occurred 'suddenly' and in an uncontrollable way. The damage of the structure array is shown in Figure 10.

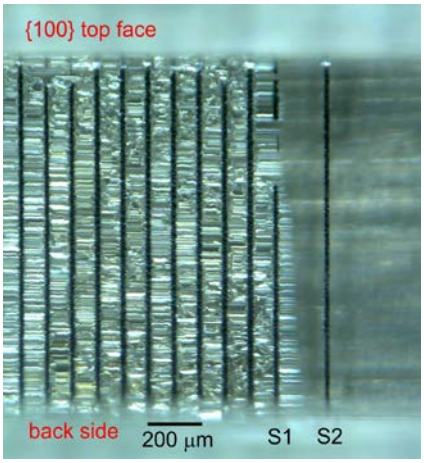

Figure 10
Array of through laser-graphitized microstructures fabricated in the 1.2-mm-thick diamond plate by visible ps-laser irradiation (E=2 μJ, f=0.5 kHz, P=1 mW, V_z=10-20 μm/s, λ=532 nm) and 'instantaneously' damaged during growth of the structure S1. Structure S2 is fabricated right after the damage of the array.

In Figure 10, ten microstructures on the left of the structure S1 have been fabricated at the conditions (E=2-3 μJ, f=0.5-1 kHz, V_z=10-20 μm/s, λ=532 nm) which provided each structure to be formed through the plate at 100 μm spacing, with no visible crack formation near the microstructures, similar to the data reported in [1]. Making the structure S1 (at E=2 μJ, f=0.5 kHz, V_z=10 μm/s) has resulted, at ≈ 800 μm from the BS (see a break point), in a 'catastrophic' growth of the cracks in the direction normal to the produced microstructures and in an 'instantaneous' damage all over the volume across the produced microstructures – from S1 to the left. However, the structure S2 fabricated at the same conditions (as for the S1) and 200 μm spacing, showed no damage again around laser-graphitized microstructure. So, we suggest that high internal stresses in laser-modified regions are responsible for the observed 'explosive-like' damage in the bulk of diamond during ps-laser microstructuring.

We have made estimations of the internal stresses generated in diamond as a result of bulk structure transformations. A scheme of modeling of internal stresses in the system 'graphitized cylinder – in – diamond' is shown in Figure 11. In the modeling we assume that a cylinder of radius R (infinite along Z axis) is taken out from diamond, then 'graphitized', and finally it is put back into diamond. An objective of modeling was to see how the properties of laser-modified material (ρ_1, E_1, υ_1) affect the resulting internal stresses in the system (ρ_1 is the material density, E_1 is the Young's modulus, and υ_1 is the Poisson's ratio).

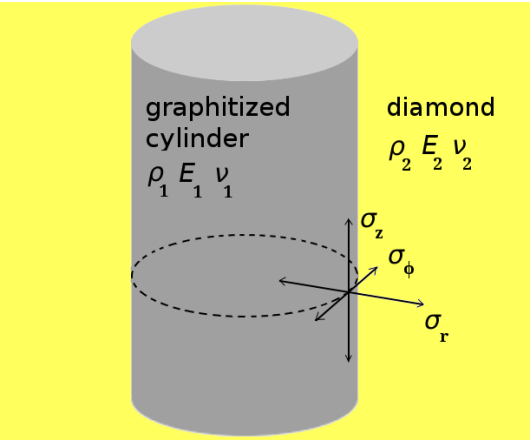

Figure 11
Scheme of modeling of internal stresses in the system 'graphitized cylinder – in – diamond'.

Using Hooke's law for isotropic materials (see, e.g. [19]) in the form in which the strain is expressed in terms of the stress tensor and assuming certain equilibrium and boundary conditions, we get the following analytical expressions for the stresses inside the graphitized cylinder and in the surrounding diamond:

$$\sigma_{1r} = \sigma_{1\phi} = -C(1+k\nu_1)E_2 = const,$$
$$\sigma_{1z} = -C\big((k+\nu_1(2-k))E_2 + (1+\nu_2)E_1\big) = const,$$
$$C = \frac{(k-1)E_1}{kE_2(1-\nu_1-2\nu_1^2)+E_1(1+\nu_2)}. \quad (1)$$

where $k=(\rho_2/\rho_1)^{1/3}$,

$$\sigma_{2r}(r) = -\sigma_{2\phi}(r) = \sigma_{1r}\frac{R^2}{r^2}, \sigma_{2z} = 0 \quad (2)$$

We then assume the stresses inside the cylinder equal for all axes: $\sigma_{1r} = \sigma_{1\phi} = \sigma_{1z}$, for which the expression for the stresses is very lengthy, and the eq.(2) is valid.

Two types of material of the graphitized cylinder are selected for modeling. The first material is tetrahedral amorphous carbon (ta-C) (based on the Raman study, see Fig.6) which is dense and hard, with the density of ρ_1=2.9-3.1 g/cm^3 and Young's modulus E_1=550-750 GPa (see refs. [10, 20-21]). Below it is called diamond-like carbon (DLC). The second material is isotropic pyrocarbon (pyrographite) which is less dense (ρ_1=2.2 g/cm^3) and soft (E_1=28 GPa) [22]. For diamond we take: ρ_2=3.5 g/cm^3, E_2=1050 GPa, υ_2=0.07 [18]. The results of calculations of internal stresses are given in Table 1. An important conclusion is that the transformation from diamond to hard amorphous carbon results in considerably higher internal stresses than the transformation to the soft graphitic material, though the $\Delta\rho=\rho_1-\rho_2$ is considerably smaller. So, the laser damage is supposed to result from the diamond-to-DLC transition while the explosive-like character of crack growth and energy release is a point to be clarified.

Table1. Stresses in the system 'graphitized cylinder-in-diamond'

material	ρ_1, g/cm^3	E_1, GPa	υ_1	$\lvert\sigma_1\rvert$, GPa
DLC1	3.1	750	0.12	24.0
DLC2	3.1	550	0.12	19.6
DLC3	2.9	550	0.12	30
Isotropic pyrocarbon	2.2	28	0.2	6.8

Conclusions

Crystallographic-plane dependence of bulk modifications in single-crystal diamond is an important factor in microstructuring, its mechanism is based on the strength anisotropy of diamond; microprocessing limitations are evident.

High-order Stokes Raman lasing is demonstrated during UV ps-laser irradiation and bulk modifications of single-crystal diamond. The

formation of a bulk microstructure in diamond was found to result in dramatic changes in the PL spectra and SRS lasing.

Important limitations (for diamond applications) are due to high internal stresses in laser-modified regions leading to 'uncontrollable' damage of the diamond single crystals.

Acknowledgements

The work was supported by the SNSF project IZ73Z0-128088/1.

References

[1] S.M. Pimenov, I.I. Vlasov, A.A. Khomich, B. Neuenschwander, M. Muralt, V. Romano (2011), Picosecond-laser-induced structural modifications in the bulk of single-crystal diamond, Applied Physics A 105, 673-677

[2] K. Weingarten (2009), High energy picosecond lasers: ready for prime time, Laser Technik Journal 6(3), 51-54

[3] B. Neuenschwander, G.F.Bucher, C. Nussbaum, B. Joss, M. Muralt, U.W. Hunziker, P. Schuetz (2010), Processing of metals and dielectric materials with ps-laserpulses: results, strategies, limitations and needs, Proc. SPIE 7584, 75840R

[4] www.e6cvd.com

[5] A. Wotherspoon, J.W. Steeds, P. Coleman, D. Wolverson, J. Davies, S. Lawson, J. Butler (2002), Photoluminescence studies of type IIa and nitrogen doped CVD diamond, Diamond Related Materials 11, 692-696

[6] T.V. Kononenko, M. Meier, M.S. Komlenok, S.M. Pimenov, V. Romano, V.P. Pashinin, V.I. Konov (2008), Microstructuring of diamond bulk by IR femtosecond laser pulses, Applied Physics A 90, 645-651

[7] T.V. Kononenko, M.S. Komlenok, V.P. Pashinin, S.M. Pimenov, V.I. Konov, M. Neff, V. Romano, W. Lüthy (2009), Femtosecond laser microstructuring in the bulk of diamond, Diamond & Related Materials 18, 196–199.

[8] R.H. Telling, C.J. Pickard, M.C. Payne, and J. E. Field (2000), Theoretical strength and cleavage of diamond, Phys. Rev. Lett. 84, 5160-5163

[9] L. Pastewka, S. Moser, P. Gumbsch, and M. Moseler (2011), Anisotropic mechanical amorphization drives wear in diamond, Nature Materials 10, 34–38

[10] A.C. Ferrari, B. Kleinsorge, N.A. Morrison, A. Hart, V. Stolojan, J. Robertson (1999), Stress reduction and bond stability during thermal annealing of tetrahedral amorphous carbon, J. Appl. Phys. 85, 7191-7197

[11] J.W. Steeds, W. Sullivan, A. Wotherspoon and J.M. Hayes (2009), Long-range migration of intrinsic defects during irradiation or implantation, J. Phys.: Condens. Matter 21, 364219

[12] A.K. McQuillan, W.R.L. Clements, and B.P. Stoicheff (1970), Stimulated Raman emission in diamond: Spectrum, gain, and angular distribution of intensity, Phys. Rev. A 1, 628-635

[13] A.A. Kaminskii, R.J. Hemley, J. Lai, C.S. Yan, H.K. Mao, V.G. Ralchenko, H.J. Eichler, and H. Rhee (2007), High-order stimulated Raman scattering in CVD single crystal diamond, Laser Phys. Lett. 4, 350–353

[14] T.T. Basiev, A.A. Sobol, P.G. Zverev, V.V. Osiko, R.C. Powell (1999), Comparative spontaneous Raman spectroscopy of crystals for Raman lasers, Appl. Opt. 38, 594-598

[15] R.P. Mildren, A. Sabella (2009), Highly efficient diamond Raman laser, Opt. Lett. 34, 2811-2813

[16] D. J. Spence, E. Granados, R. P. Mildren (2010), Mode-locked picosecond diamond Raman laser, Opt. Lett. 35, 556-558

[17] E. Granados, D. J. Spence, R. P. Mildren (2011), Deep ultraviolet diamond Raman laser, Optics Express 19, 10857-10863

[18] J.E. Field, C.S.J. Pickles (1996), Strength, fracture and friction properties of diamond, Diamond and Related Materials 5, 625-634

[19] L.D. Landau and E.M. Lifshitz (1970), Theory of Elasticity (Volume 7 of A Course of Theoretical Physics) Pergamon Press

[20] T.A.Friedmann, J.P. Sullivan, J.A. Knapp, D.R. Tallant, D.M. Follstaedt, D.L. Medlin, P.B. Mirkarimi (1997), Thick stress-free amorphous tetrahedral carbon films with hardness near that of diamond, Appl. Phys. Lett. 71, 3820-3822.

[21] A.C. Ferrari, J. Robertson, M.G. Beghi, C.E. Botani, R. Ferulano, R. Pastorelli (1999), Elastic constants of tetrahedral amorphous carbon films by surface Brillouin scattering, Appl. Phys. Lett. 75, 1893-1895

[22] H.O. Pierson (1993), Handbook of carbon, graphite, diamond and fullerenes (Properties, processing and applications), P.A. Thrower, Editor-in-Chief. Noyes Publications (Park Ridge, New Jersey, USA), 1993, pp. 417